Original Research Article

Age or ischemia uncouples the blood flow response, tissue acidosis, and the direct current potential signature of spreading depolarization in the rat brain

Ákos Menyhárt, Dániel Zölei-Szénási, Tamás Puskás, Péter Makra, Ferenc Bari, Eszter Farkas*

Department of Medical Physics and Informatics, Faculty of Medicine & Faculty of Science and Informatics, University of Szeged, H-6720 Szeged, Korányi fasor 9, Hungary

Author contributions:

Á.M.: acquisition, analysis and interpretation of data, drafting a significant portion of the manuscript; D.Z-S.: acquisition and analysis of data; T.P.: analysis of data; P.M.: analysis of data; F.B: drafting a significant portion of the manuscript; E.F.: conception and design, acquisition, analysis and interpretation of data, drafting a significant portion of the manuscript and figures.

Running head: Metabolic coupling with spreading depolarization

***Corresponding author:**

Eszter Farkas, Ph.D.
Department of Medical Physics and Informatics
Faculty of Medicine, and Faculty of Science and Informatics
University of Szeged
H-6720 Szeged, Korányi fasor 9, Hungary
Tel.: +36 62 545 829, E-mail: farkas.eszter.1@med.u-szeged.hu

Abstract

Spreading depolarization (SD) events contribute to lesion maturation in the acutely injured human brain. Neurodegeneration related to SD is thought to be caused by the insufficiency of the cerebral blood flow (CBF) response; yet, the mediators of the CBF response, or their deficiency in the aged or ischemic cerebral cortex remain the target of intensive research. Here we postulate that tissue pH effectively modulates the magnitude of hyperemia in response to SD, which coupling is prone to be dysfunctional in the aged or ischemic cerebral cortex. To test this hypothesis, we conducted systematic correlation analysis between the direct current (DC) potential signature of SD, SD-associated tissue acidosis and the hyperemic element of the CBF response, in the isoflurane-anesthetized, young or old, and intact or ischemic rat cerebral cortex. The data demonstrate that the amplitude of the SD-related DC potential shift, tissue acidosis and hyperemia are tightly coupled in the young intact cortex; ischemia and old age uncouples the amplitude of hyperemia from the amplitude of the DC potential shift and acidosis; the duration of the DC potential shift, hyperemia and acidosis positively correlate under ischemia alone; and old age disproportionally elongates the duration of acidosis with respect to the DC potential shift and hyperemia under ischemia. The coincidence of the variables supports the view that local CBF regulation with SD must have an effective metabolic component, which becomes dysfunctional with age or under ischemia. Finally, the known age-related acceleration of ischemic neurodegeneration may be promoted by exaggerated tissue acidosis.

Key words

aging, cerebral blood flow, cerebral ischemia, metabolic coupling, spreading depolarization

New & Noteworthy

The hyperemic element of the cerebral blood flow response to spreading depolarization is effectively modulated by tissue pH in the young intact rat cerebral cortex. This coupling becomes dysfunctional with age or under ischemia, and tissue acidosis lasts disproportionally longer in the aged cortex, making the tissue increasingly more vulnerable.

Introduction

Spontaneously occurring spreading depolarization (SD) events have been implicated in the maturation of ischemic brain infarction and the development of secondary injury after subarachnoid hemorrhage and traumatic brain injury [14,27]. In addition, SD events have been recently proposed to be “a universal principle of cortical lesion development” in the cerebral gray matter [11,26]. Waves of SD that propagate over the cerebral cortex at a low rate of a few millimeters per minute involve a critical mass of neurons and glia cells at any point of the wave front as the depolarization event is spreading, and generate a metabolic demand for the nervous tissue to regain an electrophysiological resting state [13,37]. The metabolic challenge is reflected by a transient tissue acidosis spatiotemporally coupled with SD [42,43], and answered by a typical cerebral blood flow (CBF) response including a pronounced transient hyperemic component that evolves conditional upon the actual energetic status of the tissue [2,10].

The regulation of the CBF response to SD has been a target of intensive research, but its nature and mediators have not been unequivocally identified. First, the hyperemic component of the CBF response was perceived as reactive hyperemia predominantly driven by metabovascular coupling [36]. This view was later revised, and the increased perfusion in response to SD was assumed to be functional hyperemia mediated by neurovascular coupling [2]. In a recent study, we found in the cerebral cortex of young adult rats, that the higher amplitude of tissue acidosis with SD strongly correlated with the higher amplitude of the SD-related hyperemia [42], supporting the view of a potential metabolic coupling. This observation has prompted us to hypothesize that the intensity of depolarization must be proportional to the magnitude of the subsequent tissue acidosis, which, in turn, should drive the evolution of the ensuing hyperemia with SD. Indeed, tissue pH has long been proposed to control CBF [35,54] and was shown to mediate functional hyperemia associated with seizure activity [33]. Therefore, we set out here to systematically explore meaningful associations between the kinetics of the typical DC potential signature of SD, the related variations in tissue pH, and the hyperemic component of the CBF response, in order to shed light on potential patterns of coupling.

With aging, SDs propagating over the ischemic cerebral cortex appear to be increasingly more harmful, as evidenced by the enlarged surface of cortical tissue involved in prolonged depolarization [7]. Repolarization may be delayed in the aging cortex because recovery from the SD-related acidosis is considerably hampered by age [42], and the SD-related hyperemia becomes insufficient and often seriously impaired (i.e. spreading ischemia) [7,18,41,42]. All these together have been considered to indicate or promote the conversion of the ischemic penumbra to the irreversibly damaged core region [26,42], a pathophysiological process accelerated in the aged brain [1,7,16,58].

Despite the age-related weakening of hyperemia in response to SD, there is no evidence that the intensity of the underlying depolarization would proportionally be smaller. This raises the assumption that age weakens the coupling between SD and the associated hyperemia. Such a hypothesis is reasonable, since age has been shown to impair neurovascular coupling with somatosensory stimulation, probably due to the increased production of NADPH oxidase-derived reactive oxygen species in the neurovascular domain [46,61]. Likewise, neurovascular coupling was found dysfunctional immediately or days after cerebral ischemia onset, as indicated by failing functional hyperemia in response to preserved neuronal activity corresponding to somatosensory stimulation [31]. Hence, we sought to evaluate how ischemia or age would influence the perceived association between SD, tissue acidosis and CBF.

Materials and Methods

General procedures

The experimental procedures were approved by the National Food Chain Safety and Animal Health Directorate of Csongrád County, Hungary. The procedures conformed to the guidelines of the Scientific Committee of Animal Experimentation of the Hungarian Academy of Sciences (updated Law and Regulations on Animal Protection: 40/2013. (II. 14.) Gov. of Hungary), following the EU Directive 2010/63/EU on the protection of animals used for scientific purposes.

Procedures were identical to those reported recently [42]. Briefly, isoflurane-anesthetized (1.1-1.3 % isoflurane in N_2O:O_2, 70%:30%), spontaneously breathing young adult (2 month-old, n=20) and old (18-20 month-old, n=18) male Sprague-Dawley rats were used. Mean arterial blood pressure was continuously monitored via a femoral artery cannule throughout the experiments, which was also used for the withdrawal of blood samples for arterial blood gas analysis. Together with the parallel, live display of the electrocorticogram, the mean arterial blood pressure signal was also used as feed-back to adjust and keep anesthesia at an optimal level. The experimental protocol consisted of three, subsequent phases: (i) a baseline period of 50 min followed by (ii) incomplete, global forebrain ischemia induced by the transient, bilateral occlusion of the common carotid arteries, and (iii) concluded an hour later by reperfusion, initiated by the release of the carotid arteries. The experiments were terminated by the overdose of the anesthetic agent. Three SDs were triggered during each phase of the experiments, with the topical application of 1M KCl at an inter-SD interval of 15 minutes.

For the monitoring of tissue pH and CBF, the animals were assigned to two series of experiments. In *Series 1*, a pH-sensitive microelectrode was implanted into the cerebral cortex and a laser Doppler probe was positioned near the penetration site of the microelectrode to assess CBF variations (n=17). In *Series 2*, a large, closed cranial window was created over the parietal cortex for the imaging of tissue pH and CBF in the upper layers of the cortex (n=20).

Series 1

As presented earlier [42], two small, open craniotomies were drilled in the right parietal bone. Ion-sensitive microelectrodes were constructed according to Voipio and Kaila [65]. In each experiment, a pH-sensitive microelectrode together with a reference electrode was lowered into the cortex with their tips positioned as near as possible; an Ag/AgCl electrode implanted under the skin of the animal's neck served as common ground (n=17). The reference electrode acquired DC potential. The raw signals were recorded at 1 kHz, filtered, conditioned, amplified (AD549LH, Analog Devices, Norwood, MA, USA; NL834, NL 820, NL125, NL530, Digitimer Ltd., U.K.) and converted to digital signals (MP 150 and AcqKnowledge 4.2.0, Biopac

Systems, Inc. USA) as detailed previously [42]. Extracellular pH (pHe) changes were expressed in mV to be translated into pH units offline, using least squares linear regression. To monitor changes in local CBF, a laser-Doppler needle probe (Probe 403 connected to PeriFlux 5000; Perimed AB, Sweden) was positioned adjacent to the intra-cortical microelectrodes (n=14). The laser-Doppler flow (LDF) signal was digitized and displayed together with the DC potential and pH signals. The caudal craniotomy was later used for SD elicitation by placing a 1M KCl-soaked cotton ball on the exposed cortical surface. The cotton ball was removed and the cranial window rinsed with artificial cerebrospinal fluid (aCSF; composition in mM concentrations: 126.6 NaCl, 3 KCl, 1.5 CaCl2, 1.2 MgCl, 24.5 NaHCO3, 6.7 urea, 3.7 glucose bubbled with 95 % O2 and 5 % CO2 to achieve a constant pH of 7.4) immediately after each successful SD elicitation.

Series 2

The imaging experiments relied on a closed cranial window preparation (size: 4.5 × 4.5 mm) that was created over the right parietal cortex of the rats [19,45]. The cranial window incorporated a glass capillary at the caudomedial edge, used to eject 1 µl 1M KCl to evoke SD, and a glass capillary microelectrode near the lateral edge of the craniotomy to acquire DC potential with reference to an Ag/AgCl neck electrode. Signal amplification, conditioning and filtering for the DC signal was achieved as published earlier [30].

Imaging relied on infrastructure developed and updated in our lab [17,42], and followed established protocols [42]. Briefly, the fluorescent pH indicator Neutral Red (3-amino-m-dimethylamino-2-methylphenazine hydrochloride, NR, Sigma-Aldrich) was dissolved in saline (35 mM), and administered i.p. (2 x 1 ml) 30-35 min prior to the start of imaging [34]. Neutral Red incorporated by the nervous tissue was excited with a light emitting diode (LED; 530 nm peak wavelength, SLS-0304-A, Mightex Systems, Pleasanton, CA, USA; bandpass filter 3RD 540-570 nm, Omega Optical Inc. Brattleboro, VT, USA; illumination 100 ms/s), and the emitted fluorescence was captured with a monochrome CCD camera (Pantera 1M30, DALSA, Gröbenzell, Germany) attached to a stereomicroscope (MZ12.5, Leica Microsystems, Wetzlar, Germany) after proper bandpass filtering (50 nm wide, centered on 625 nm, XF3413-625QM50; Omega Optical Inc. Brattleboro, VT, USA). The stereomicroscope was equipped with a 1:1 binocular/video-tube beam splitter to

allow the mounting of a second camera, which, synchronous with NR images, captured green intrinsic optical signal (IOS) (exposure: 100 ms/s), and was additionally used to generate CBF maps utilizing laser speckle contrast analysis (LASCA) [45]. For the latter purpose, a laser diode illuminated the cortical surface (HL6545MG, Thorlabs Inc., New Jersey, USA; 120 mW; 660 nm emission wavelength; power supply: LDTC0520, Wavelength Electronics, Inc., Bozeman, USA), the illumination being synchronized with camera exposure (1 frame/second; 2 ms for illumination and 100 ms for exposure). A dedicated program written in LabVIEW environment coordinated the illuminations by various light sources and the exposures of the two cameras. Image processing including the conversion of raw speckle images to flow maps and correction of NR fluorescence for absorption by hemoglobin and dye bleaching were computed offline in MATLAB (The MathWorks Inc., Natick, MA, USA) [9,56].

Local changes in NR fluorescence intensity and CBF with time were extracted by placing regions of interest (ROIs) of ~70 × 70 µm at selected sites devoid of any blood vessels visible in the images. CBF recordings delivered by LDF or LASCA were expressed relative to baseline by using the average CBF value of the first 240 s of baseline (100%) and the recorded biological zero obtained after terminating each experiment (0%) as reference points.

Data processing and analysis

Experiments were selected for data analysis based on the quality of the recordings: experiments in which all synchronous variables (i.e. DC potential, tissue pH and CBF) were of high quality (i.e. devoid of noise or artifact during SD events) to allow reliable quantitation were processed.

The duration and relative amplitude of the negative DC potential shift indicative of SD, of the related acidosis and of hyperemia were measured. For group comparisons, data are given as mean±stdev, and were statistically tested by a two-way analysis of variance (ANOVA) paradigm (factors: phase of experiments, and age of animals) of the software SPSS (IBM SPSS Statistics for Windows, Version 22.0, IBM Corp.) Correlation analysis between variables was achieved by a two-tailed Pearson correlation test run in the same statistical

186 software. Levels of significance were determined and labeled as $p<0.05$* and $p<0.01$**. Relevant statistical
187 methods are also provided in detail in each Figure legend.
188
189 **Results**
190
191 In our current experiments, the amplitude of the negative DC potential shift corresponding to SDs fell on
192 a continuum as demonstrated in Figure 1, ranging between 0.99-19.44 mV in *Series 1*. SDs with various DC
193 potential shift amplitude were evenly distributed between age groups and phases of the experiments,
194 establishing no particular impact of age or ischemia (two-way ANOVA: $F_{age}=0.460$, $F_{phase}=0.773$).
195 For the evaluation of the metabolic consequences of SDs, the association between the amplitude and
196 duration of the DC potential shift, related acidosis, and hyperemia was analyzed in detail in *Series 1* (Fig. 2-
197 4). During baseline, in the young animals, the amplitude of all three variables was tightly coupled (e.g. DC
198 potential shift & hyperemia: r=0.819*) (Fig. 2B-C), while their duration appeared to be unrelated to each
199 other (e.g. DC potential shift & hyperemia: r=0.176) (Fig. 2E-F).
200 Under ischemia, the amplitude of hyperemia dissociated from the amplitude of both the DC potential
201 shift and acidosis (r=0.236 and r=0.429, respectively), and remained uncoupled during reperfusion, as well
202 (Fig. 2B-C). At the same time, the positive correlation between the amplitude of the DC potential shift and
203 acidosis continued to be unaffected by ischemia (r=0.789**) (Fig. 2B). The durations of the three variables
204 independent under baseline became interrelated over the ischemic phase (e.g. DC potential shift & acidosis:
205 r=0.935**), and lost correlation again during reperfusion (Fig. 2E-F).
206 Aging exerted a discernible effect on the amplitude of the three variables during baseline (Fig. 3).
207 Strikingly similar to the impact of ischemia, old age uncoupled the amplitude of hyperemia from that of the
208 DC potential shift and acidosis (r=0.221 and r=0.249, respectively), while left the amplitude of the DC
209 potential shift and acidosis strongly correlating (r=0.998**) comparable to young age (Fig. 3B-C).
210 Finally, aging dissociated the duration of acidosis from the duration of the DC potential shift and
211 hyperemia under ischemia (r=0.482 and r=0.286, respectively), while did not alter the baseline association

between the length of the DC potential shift and hyperemia (r=0.657*) (Fig. 4B). The age-related uncoupling of acidosis from the other variables was clearly due to the marked elongation of the duration of acidosis relative to the other variables in the old group (Fig. 4C). More specifically, the length of acidosis was approximately 40 % longer than the DC potential shift in the young animals, while almost doubled relative to the duration of the DC potential shift in the old group. Remarkably, the duration of acidosis was relatively shorter than the duration of hyperemia in the young group, but exceeded the duration of hyperemia in the old animals (Fig. 4C). Finally, it is noteworthy that the relative duration of hyperemia was gradually decreasing (195 % → 172 % → 167 %, young baseline → young ischemia → old ischemia), while the relative duration of acidosis was increasing with ischemia and age (127 % → 140 % → 192 %, young baseline → young ischemia → old ischemia) (Fig. 4C).

Examining the videos obtained with green IOS, NR imaging and LASCA in *Series 2*, it has become clear that SDs with small amplitude as seen on DC potential traces must designate extinguishing SD waves. In the representative example given in Figure 5, the optical signals of CBF, tissue pH and green IOS revealed that the SD diminished halfway over its course in the field of view. Yet, the electrode positioned about 500 µm distant to the rim of the aborting SD still indicated a small negative DC potential shift, even though the optical signature of SD did not reach that site. We hypothesized, that such SD events could become gradually smaller and then cease to propagate because they travel against a lowering tissue pH gradient reported to inhibit SD [58,60]. Indeed, brighter NR fluorescence associated with lower pH in Figure $4A_2$ corresponds with the area where SD came to a halt. When SD events evoked during baseline in *Series 1* were sorted on the basis of DC potential shift amplitude (i.e. smaller than 5 mV and greater than 5 mV) (Fig. 6A), tissue pH proved to be significantly more acidic prior to SDs with small DC potential shift amplitude (pH 7.20±0.04 vs. 7.31±0.03) (Fig. 6B). In further support, a strong positive correlation was established between tissue pH prior to SD and the DC potential shift amplitude with SD (r=0.909**), which was abolished by ischemia (r=0.244), and re-established during reperfusion (r=0.739*) (Fig. 6C-D).

In summary, our correlation analyses demonstrate that (i) low tissue pH in the intact cortex predicts small DC potential shift amplitude with SD, indicative of SD vanishing; (ii) the amplitude of the SD-related DC

potential shift, tissue acidosis and hyperemia are tightly coupled in the young intact cortex; (iii) ischemia and old age uncouples the amplitude of hyperemia from the amplitude of the DC potential shift and acidosis; (iv) the duration of the DC potential shift, hyperemia and acidosis positively correlate under ischemia in young animals; and (v) old age dissociates the duration of acidosis from that of the DC potential shift and hyperemia under ischemia.

Discussion

The recording of the DC potential is a conventional, robust experimental technique, which has been routinely used for over seven decades to identify SD occurrence in the cerebral cortex of anesthetized animals, *in vitro* brain slice preparations, and most recently, in brain injury patients [12,28,55]. The DC potential shift representing the sum of neuronal and glial depolarization reflects gross ionic translocations between the intra-and extracellular compartments, and correlates well with the extracellular surge of K^+ with SD [49,51,55]. Recurrent SDs in the injured brain of patients are perceived to mark and to exacerbate metabolic failure and excitotoxic injury [10,11,26], especially because the long cumulative duration of recurrent SDs has emerged as an early indicator of delayed ischemic brain damage [11,14]. Still, it has remained largely unexplored whether the SD-related metabolic challenge could possibly be estimated by examining and evaluating the quantitative characteristics of the negative DC potential shift of individual SD events. More importantly, proving direct coupling between depolarization, tissue pH variations and the CBF response with SD should foster the understanding of the pathophysiological sequence and significance of events initiated by SD in the injured brain.

The degree of tissue acidosis is related to the negative DC potential shift with spreading depolarization

The recording of the DC potential is an inherent component of the assessment of tissue pH variations with the use of ion-sensitive microelectrodes [65], which, therefore, allows the direct comparison of the two synchronous signals. Still, thorough correlation analysis between quantitative features of the DC potential

shift and acidosis with SD has not been presented. Investigators exploring tissue pH changes with SD relying on microelectrodes focused on the cellular mechanisms of pH regulation [43], or examined the close relation between the elevation of lactate and the decrease of tissue pH [52]. Later *in vitro* studies concentrated on the short-lasting alkalotic shift that precedes the SD-related acidosis with the purpose to dissect its role in the potential facilitation of SD occurrence in the ischemic nervous tissue, and left the subsequent phase of longer lasting acidosis unattended [40,60].

Here we present that the amplitude of the SD-related DC potential shift and that of acidosis strongly correlate in the intact rodent cortex, and this association persists steadily under ischemia and in the aged brain. These findings suggest that the positive coupling between the amplitude of the DC potential shift and subsequent acidosis with SD is highly conserved, and a larger shift of the DC potential predicts a more pronounced acidic peak with SD. Assuming that a greater shift in the DC potential indicates more intensive depolarization, and accepting that neuronal activity is directly followed by an increase in intra- and extracellular acid load, as shown in experimental models as well as by non-invasive imaging of the human brain [6,39], it is reasonable to anticipate that a larger DC potential shift as shown here yields deeper acidosis.

Ischemia or aging impairs the coupling between spreading depolarization and the associated cerebral blood flow response

Our correlation analysis here demonstrates that the peak of hyperemia in response to SD is directly proportional to the amplitude of the DC potential shift and that of acidosis in the intact cortex. This result is consistent with the outcome of fundamental positron emission tomography studies, which concluded that local CBF was linearly coupled with neuronal activity in response to visual stimulation under physiological conditions [21]. Furthermore, a recent report has also confirmed this association by showing larger whisker stimulation-evoked CBF responses together with the intensification of neuronal activity in the intact rodent cortex [38]. Finally, it appears that tissue pH decreasing transiently with SD can modulate the amplitude of the ensuing CBF response (Fig. 7). The perceived causality would support the idea that local CBF regulation

with SD must have an effective metabolic component [36], in addition to the more accepted neurovascular coupling hypothesis [2].

We have found that the correlation between the amplitude of hyperemia and that of the DC potential shift or acidosis with SD becomes lost under ischemia. Ischemia is known to impair neurovascular coupling as demonstrated by the attenuation of functional hyperemia to forepaw stimulation in rodent models [31]. Likewise, ischemia significantly reduced the amplitude of hyperemia in response to SD, which has been systematically evaluated against SD-related hyperemia recorded in the intact cortex [30,41,42,64]. At the same time, the amplitude of the SD-related DC potential shift was shown to be resistant to ischemia [41]. These data, fortified by the present analyses, demonstrate that even though SDs are as intense under ischemia as in the intact cortex, the CBF response becomes impaired, clearly confirming dysfunctional coupling between the two variables. In addition, we show here that not only ischemia but also healthy aging dissociates the amplitude of hyperemia from that of the DC potential shift with SD. This phenomenon is highly consistent with the well-studied adverse effect of aging on the efficacy of neurovascular coupling, which was linked to the generation of free radicals and oxidative stress [46,62].

Aging disproportionately increases the duration of tissue acidosis with spreading depolarization

We reported previously that longer depression of the electrocorticogram (ECoG) or a longer DC potential shift with SD was associated with longer hyperemia, and argued that the return of CBF to baseline after peak hyperemia was postponed by the continuing energy need of the tissue, as reflected by the sustained depolarization [30,41]. However, whether this association was valid for the intact as well as for the ischemic condition has not been distinguished. Here we show that the longer duration of hyperemia to SD coincides with longer depolarization, as well as with a longer-lasting acidosis in the ischemic brain only (Fig. 2E). One plausible reason for the lack of correspondence between the length of hyperemia and the DC potential shift in the intact cortex may be that hyperemia lasts disproportionately longer in the intact than in the ischemic condition (Fig. 4C). This would be consistent with the notion that the CBF response to SD creates luxury perfusion in the cortex that receives uninterrupted blood supply [2].

A novel observation of this study suggests that aging disrupts the correspondence of acidosis duration with the duration of the DC potential shift and hyperemia with SD (Fig. 4B). At closer inspection, the relative length of acidosis increases excessively in the aged ischemic brain, which accounts for the loss of correlation (Fig. 4C). Acid load with SD was suggested to be caused by the accumulation of lactate [20,43,52], which is readily cleared into the blood stream within minutes after SD is triggered in the intact young rodent cortex [8]. Considering these data, it is conceivable that the sustained acidosis with SD in the aged brain is caused by decelerated lactate efflux through the blood-brain barrier. The consequences of the exaggerated duration of acidosis are thought to be twofold. First, the threshold of acid-induced cell death was shown to be reduced with the prolongation of acid exposure [44], which may put the aging brain at a higher risk for acid-induced ischemic neurodegeneration [32]. Second, considering that acidosis outlasts hyperemia as seen here, the mismatch between these variables is perceived to indicate accentuated metabolic crisis instigated by SD in the aged brain.

Small DC potential amplitude corresponds with the extinguishing edge of spreading depolarizations

As the DC potential shift indicative of SD was comprehensively analyzed here, a seemingly technical issue that has been dormant for some time was addressed. We and others regularly encounter atypical SD-associated, negative DC shifts in the intact and injured cortex, which are rather small in amplitude. These events (Fig. 1A) give rise to uncertainty as to whether the small DC potential shift should be considered to indicate a true SD wave. Moreover, the metabolic consequences of these obscure events on the DC potential traces are of interest to assess their significance and injurious potential, but have not yet been examined. Therefore we also aimed to identify the origin and nature of the small, atypical DC potential shifts that occasionally evolve spontaneously in the injured cortex, or in response to experimental SD elicitation.

The typical size of the SD-related negative DC potential shift as measured by an intracortical electrode relative to a distant ground is 15-30 mV [55]. The occasional, rather small amplitude (i.e. < 5 mV) of a few SD-related DC potential shifts acquired via the same electrode, within the same preparation that also delivers typically large signals with other SDs, has been puzzling to investigators who rely on the DC potential

signature to confirm SD occurrence. The ambiguity as to whether a DC potential shift of small amplitude should be considered to reflect the actual evolution of an SD can be resolved by formulating the restriction that a DC potential variation indicates an SD event only when its amplitude exceeds a given value. However, what the threshold value should be is difficult to justify, particularly in view of our present data showing an uninterrupted spectrum of the DC potential shift amplitude within the same set of experiments (Fig. 1B). This dilemma seems to be settled by our imaging studies, which reveal the spatial in addition to the temporal pattern of SD propagation. By the combination of DC potential recording with optical imaging, here we demonstrate that extinguishing SDs leave their signature on the DC potential trace as transient negative shifts of small amplitude (Fig. 5). This is supported by our previous observations achieved by imaging SD-related membrane potential changes with a voltage-sensitive dye, whose fluorescence is analogous to that of the DC potential [19]. We showed that the voltage-sensitive dye signature of SD was decreasing gradually in amplitude as an SD wave was diminishing over its course, together with decreasing magnitude of the coupled hemodynamic response [4]. All things considered, a small transient negative DC potential shift recorded under identical experimental conditions that also deliver large DC potential shifts is assumed to represent SD events, but obviously corresponds to the phase of the wave where SD is aborting as it propagates over the cortex. The SD's metabolic impact at the site of the recording electrode appears to be proportional to the small size of the negative DC potential shift; however this provides no evidence for the metabolic impact of the same SD at its full magnitude, closer to the site of elicitation, before arriving at the recording site.

Does low tissue pH predict small DC potential amplitude with spreading depolarization?

It has been long accepted that low pH hampers the elicitation and propagation of SD, which notion was corroborated by the delayed occurrence and slower rate of propagation of SD in brain slices exposed to an acidic medium [58,60]. The reason for SD suppression by low pH was suggested to be the inhibition of the NMDA receptors by extracellular protons [57], or the modulation of the conductance and gating properties of voltage-gated K^+, Na^+ and Ca^{2+} channels [59]. Here we present data obtained *in vivo* that lower tissue pH

coincides with the smaller amplitude of the DC potential shift with arising SDs, but this association is valid only in the normally perfused cortex and is lost under ischemia.

Taken our argument proposing that a smaller DC potential amplitude corresponds with an SD in its diminishing phase, we can postulate that SD events do not only propagate slower at lower, albeit physiological pH [60], but also cover a shorter distance before coming to a halt. The imaging data presented here convincingly support this idea (Fig. 5).

In view of this suggestion, it is interesting to observe that lower pH does not predict smaller DC potential shift – and thus supposedly shorter SD route – in the ischemic cortex. It appears that other ischemia-related factors should overrule the inhibitory effect of low pH on SD propagation. It is conceivable, for instance, that glutamate, which accumulates excessively in the ischemic nervous tissue [3,5], and has been recognized to facilitate the spreading of depolarization via NMDA receptor and voltage-gated Ca^{2+} channel activation [29,49,63], overrides tissue acidosis and promotes SD propagation. Further, extracellular K^+ has also been implicated in sustaining SD propagation [23,49], and, like glutamate, it is elevated in the ischemic tissue over physiological levels (e.g. from 2-4 mM up to 9-12 mM) that favor SD evolution [24,25]. Taken together, the inhibitory impact of tissue acidosis on SD propagation under ischemia is suggested to be negligible as compared with the facilitating role of high interstitial concentration of glutamate, potassium, or their combination.

Future perspectives

Our recent [42] and present results together implicate tissue acidosis in the mediation of SD-related neurodegeneration, especially in the aged brain, due to the poor recovery from the SD-induced acidic pH shift. Appreciating that the apparent, persisting elevation of lactate concentration accounts for the SD-related tissue acidosis [43,52,53], hampered lactate removal is thought to be a potential pathomechanism sustaining low tissue pH in the aged brain. The facilitated diffusion of lactate to the blood stream is mediated by monocarboxylic acid transporter 1 (MCT1) located on endothelial cells that form the blood-brain barrier [48]. The dysfunction of MCT1 was previously perceived to contribute to acid-related neurodegeneration in

ischemic stroke [15]. Furthermore, MCT1 expression was found strongly age-dependent in the juvenile brain [22,47], although no evidence can be retrieved to demonstrate how MCT1 expression or activity might be altered by old age. Altogether, it is conceivable that MCT1 downregulation or dysfunction at the aged blood-brain barrier could possibly impede lactate removal, thereby prolonging SD-induced lactate-acidosis, and accelerate ischemia-related neurodegeneration. If this proposition stands true, potentiating the efficacy of MCT1 function in the aged cortex under ischemia could possibly improve injury outcome after stroke. The validity of the above hypothesis should, however, be scrutinized by upcoming research.

Grants

This work was supported by grants from the National Research, Development and Innovation Office of Hungary (Grant No. K111923); the Hungarian Brain Research Program (Grant No. KTIA_13_NAP-A-I/13); the Bolyai János Research Scholarship of the Hungarian Academy of Sciences (No. BO/00327/14/5, to EF); the Economic Development and Innovation Operational Programme in Hungary co-financed by the European Union and the European Regional Development Fund (No. GINOP-2.3.2-15-2016-00006); and the EU-funded Hungarian grant No. EFOP-3.6.1-16- 2016-00008.

Disclosures

The Authors declare no perceived or potential conflict of interest, financial or otherwise.

References

1. **Ay H, Koroshetz WJ, Vangel M, Benner T, Melinosky C, Zhu M, Menezes N, Lopez CJ, Sorensen AG.** Conversion of ischemic brain tissue into infarction increases with age. *Stroke* 36(12): 2632-2636, 2005.
2. **Ayata C, Lauritzen M.** Spreading Depression, Spreading Depolarizations, and the Cerebral Vasculature. *Physiol Rev* 95(3): 953-993, 2015.
3. **Benveniste H, Drejer J, Schousboe A, Diemer NH.** Elevation of the extracellular concentrations of glutamate and aspartate in rat hippocampus during transient cerebral ischemia monitored by intracerebral microdialysis. *J Neurochem* 43(5): 1369-1374, 1984.
4. **Bere Z, Obrenovitch TP, Kozák G, Bari F, Farkas E.** Imaging reveals the focal area of spreading depolarizations and a variety of hemodynamic responses in a rat microembolic stroke model. *J Cereb Blood Flow Metab* 34(10): 1695-1705, 2014.
5. **Butcher SP, Bullock R, Graham DI, McCulloch J.** Correlation between amino acid release and neuropathologic outcome in rat brain following middle cerebral artery occlusion. *Stroke* 21(12): 1727-1733, 1990.
6. **Chesler M, Kaila K.** Modulation of pH by neuronal activity. *Trends in Neurosci* 15(10): 396-402, 1992.
7. **Clark D, Institoris A, Kozák G, Bere Z, Tuor U, Farkas E, Bari F.** Impact of aging on spreading depolarizations induced by focal brain ischemia in rats. *Neurobiol Aging* 35(12): 2803-2811, 2014.
8. **Cruz NF, Adachi K, Dienel GA.** Rapid efflux of lactate from cerebral cortex during K+ -induced spreading cortical depression. *J Cereb Blood Flow Metab* 19(4): 380-392, 1999.
9. **Domoki F, Zölei D, Oláh O, Tóth-Szuki V, Hopp B, Bari F, Smausz T.** Evaluation of laser-speckle contrast image analysis techniques in the cortical microcirculation of piglets. *Microvasc Res* 83(3): 311-317, 2012.
10. **Dreier JP.** The role of spreading depression, spreading depolarization and spreading ischemia in neurological disease. *Nat Med* 17(4): 439-447, 2011.
11. **Dreier JP, Fabricius M, Ayata C, Sakowitz OW, William Shuttleworth C, Dohmen C, Graf R, Vajkoczy P, Helbok R, Suzuki M, Schiefecker AJ, Major S, Winkler MK, Kang EJ, Milakara D, Oliveira-Ferreira AI,**

Reiffurth C, Revankar GS, Sugimoto K, Dengler NF, Hecht N, Foreman B, Feyen B, Kondziella D, Friberg CK, Piilgaard H, Rosenthal ES, Westover MB, Maslarova A, Santos E, Hertle D, Sánchez-Porras R, Jewell SL, Balança B, Platz J, Hinzman JM, Lückl J, Schoknecht K, Schöll M, Drenckhahn C, Feuerstein D, Eriksen N, Horst V, Bretz JS, Jahnke P, Scheel M, Bohner G, Rostrup E, Pakkenberg B, Heinemann U, Claassen J, Carlson AP, Kowoll CM, Lublinsky S, Chassidim Y, Shelef I, Friedman A, Brinker G, Reiner M, Kirov SA, Andrew RD, Farkas E, Güresir E, Vatter H, Chung LS, Brennan KC, Lieutaud T, Marinesco S, Maas AI, Sahuquillo J, Dahlem MA, Richter F, Herreras O, Boutelle MG, Okonkwo DO, Bullock MR, Witte OW, Martus P, van den Maagdenberg AM, Ferrari MD, Dijkhuizen RM, Shutter LA, Andaluz N, Schulte AP, MacVicar B, Watanabe T, Woitzik J, Lauritzen M, Strong AJ, Hartings JA. Recording, analysis, and interpretation of spreading depolarizations in neurointensive care: review and recommendations of the COSBID research group. *J Cereb Blood Flow Metab* (Jan 1, 2016) doi: 10.1177/0271678X16654496..

12. **Dreier JP, Major S, Manning A, Woitzik J, Drenckhahn C, Steinbrink J, Tolias C, Oliveira-Ferreira AI, Fabricius M, Hartings JA, Vajkoczy P, Lauritzen M, Dirnagl U, Bohner G, Strong AJ; COSBID study group.** Cortical spreading ischaemia is a novel process involved in ischaemic damage in patients with aneurysmal subarachnoid haemorrhage. *Brain* 132(Pt 7): 1866-1881, 2009.
13. **Dreier JP, Reiffurth C.** The stroke-migraine depolarization continuum. *Neuron* 86(4): 902-922, 2015.
14. **Dreier JP, Woitzik J, Fabricius M, Bhatia R, Major S, Drenckhahn C, Lehmann TN, Sarrafzadeh A, Willumsen L, Hartings JA, Sakowitz OW, Seemann JH, Thieme A, Lauritzen M, Strong AJ.** Delayed ischaemic neurological deficits after subarachnoid haemorrhage are associated with clusters of spreading depolarizations. *Brain* 129(Pt 12): 3224-3237, 2006.
15. **Drewes LR, Gilboe DD.** Glycolysis and the permeation of glucose and lactate in the isolated, perfused dog brain during anoxia and postanoxic recovery. *J Biol Chem* 248(7): 2489-2496, 1973.
16. **Farkas E, Bari F.** Spreading depolarization in the ischemic brain: does aging have an impact? *J Gerontol A Biol Sci Med Sci* 69(11): 1363-1370, 2014.

17. **Farkas E, Bari F, Obrenovitch TP.** Multi-modal imaging of anoxic depolarization and hemodynamic changes induced by cardiac arrest in the rat cerebral cortex. *Neuroimage* 51(2): 734-742, 2010.
18. **Farkas E, Obrenovitch TP, Institóris Á, Bari F.** Effects of early aging and cerebral hypoperfusion on spreading depression in rats. *Neurobiol Aging* 32(9): 1707-1715, 2011.
19. **Farkas E, Pratt R, Sengpiel F, Obrenovitch TP.** Direct, live imaging of cortical spreading depression and anoxic depolarisation using a fluorescent, voltage-sensitive dye. *J Cereb Blood Flow Metabol* 28(2):251-262, 2008.
20. **Feuerstein D, Backes H, Gramer M, Takagaki M, Gabel P, Kumagai T, Graf R.** Regulation of cerebral metabolism during cortical spreading depression. *J Cereb Blood Flow Metab* 36(11): 1965-1977, 2016.
21. **Fox PT, Raichle ME.** Stimulus rate determines regional brain blood flow in striate cortex. *Ann Neurol* 17(3): 303-305, 1985.
22. **Gerhart DZ, Enerson BE, Zhdankina OY, Leino RL, Drewes LR.** Expression of monocarboxylate transporter MCT1 by brain endothelium and glia in adult and suckling rats. *Am J Physiol* 273(1 Pt 1): E207-E213, 1997.
23. **Grafstein B.** Mechanism of spreading cortical depression. *J Neurophysiol* 19(2): 154-171, 1956.
24. **Hansen AJ.** The extracellular potassium concentration in brain cortex following ischemia in hypo- and hyperglycemic rats. *Acta Physiol Scand* 102(3): 324-329, 1978.
25. **Hansen AJ.** Effect of anoxia on ion distribution in the brain. *Physiol Rev* 65(1): 101-148, 1985.
26. **Hartings JA, Shuttleworth CW, Kirov SA, Ayata C, Hinzman JM, Foreman B, Andrew RD, Boutelle MG, Brennan KC, Carlson AP, Dahlem MA, Drenckhahn C, Dohmen C, Fabricius M, Farkas E, Feuerstein D, Graf R, Helbok R, Lauritzen M, Major S, Oliveira-Ferreira AI, Richter F, Rosenthal ES, Sakowitz OW, Sánchez-Porras R, Santos E, Schöll M, Strong AJ, Urbach A, Westover MB, Winkler MK, Witte OW, Woitzik J, Dreier JP.** The continuum of spreading depolarizations in acute cortical lesion development: re-examining Leão's legacy. *J Cereb Blood Flow Metabol* (Jan 1, 2016) doi: 10.1177/0271678X16654495.

27. **Hartings JA, Strong AJ, Fabricius M, Manning A, Bhatia R, Dreier JP, Mazzeo AT, Tortella FC, Bullock MR; Co-Operative Study of Brain Injury Depolarizations.** Spreading depolarizations and late secondary insults after traumatic brain injury. *J Neurotrauma* 26(11): 1857-1866, 2009.
28. **Hartings JA, Watanabe T, Dreier JP, Major S, Vendelbo L, Fabricius M.** Recovery of slow potentials in AC-coupled electrocorticography: application to spreading depolarizations in rat and human cerebral cortex. *J Neurophysiol* 102(4): 2563-2575, 2009.
29. **Hernández-Cáceres J, Macias-González R, Brozek G, Bures J.** Systemic ketamine blocks cortical spreading depression but does not delay the onset of terminal anoxic depolarization in rats. *Brain Res* 437(2): 360-364, 1987.
30. **Hertelendy P, Menyhárt Á, Makra P, Süle Z, Kiss T, Tóth G, Ivánkovits-Kiss O, Bari F, Farkas E.** Advancing age and ischemia elevate the electric threshold to elicit spreading depolarization in the cerebral cortex of young adult rats. *J Cereb Blood Flow Metabol* (Jan 1, 2016) doi: 10.1177/0271678X16643735.
31. **Jackman K, Iadecola C.** Neurovascular regulation in the ischemic brain. *Antioxid Redox Signal* 22(2): 149-160, 2015.
32. **Kraig RP, Petito CK, Plum F, Pulsinelli WA.** Hydrogen ions kill brain at concentrations reached in ischemia. *J Cereb Blood Flow Metab* 7(4): 379-386, 1987.
33. **Kuschinsky W, Wahl M.** Perivascular pH and pial arterial diameter during bicuculline induced seizures in cats. *Pflugers Arch* 382(1): 81-85, 1979.
34. **LaManna JC, McCracken KA.** The use of neutral red as an intracellular pH indicator in rat brain cortex in vivo. *Anal Biochem* 142(1): 117-125, 1984.
35. **Lassen NA.** Brain extracellular pH: the main factor controlling cerebral blood flow. *Scand J Clin Lab Invest* 22(4): 247-251, 1968.
36. **Lauritzen M.** Regional cerebral blood flow during cortical spreading depression in rat brain: increased reactive hyperperfusion in low-flow states. *Acta Neurol Scand* 75(1): 1-8, 1987.
37. **Leao AA.** Spreading depression of activity in the cerebral cortex. *J Neurophysiol* 7: 359–390, 1944.

38. **Lecrux C, Sandoe CH, Neupane S, Kropf P, Toussay X, Tong XK, Lacalle-Aurioles M, Shmuel A, Hamel E.** Impact of Altered Cholinergic Tones on the Neurovascular Coupling Response to Whisker Stimulation. *J Neurosci* 37(6): 1518-1531, 2017.

39. **Magnotta VA, Heo HY, Dlouhy BJ, Dahdaleh NS, Follmer RL, Thedens DR, Welsh MJ, Wemmie JA.** Detecting activity-evoked pH changes in human brain. *Proc Natl Acad Sci U S A* 109(21): 8270-8273, 2012.

40. **Menna G, Tong CK, Chesler M.** Extracellular pH changes and accompanying cation shifts during ouabain-induced spreading depression. *J Neurophysiol* 83(3): 1338-1345, 2000.

41. **Menyhárt Á, Makra P, Szepes BÉ, Tóth OM, Hertelendy P, Bari F, Farkas E.** High incidence of adverse cerebral blood flow responses to spreading depolarization in the aged ischemic rat brain. *Neurobiol Aging* 36(12): 3269-3277, 2015.

42. **Menyhárt Á, Zölei-Szénási D, Puskás T, Makra P, M.Tóth O, Szepes BÉ, Tóth R, Ivánkovits-Kiss O, Obrenovitch TP, Bari F, Farkas E.** Spreading depolarization remarkably exacerbates ischemia-induced tissue acidosis in the young and aged rat brain. *Scientific Reports* (April 25, 2017) doi: 10.1038/s41598-017-01284-4.

43. **Mutch WA, Hansen AJ.** Extracellular pH changes during spreading depression and cerebral ischemia: mechanisms of brain pH regulation. *J Cereb Blood Flow Metab* 4(1): 17-27, 1984.

44. **Nedergaard M, Goldman SA, Desai S, Pulsinelli WA.** Acid-induced death in neurons and glia. *J Neurosci* 11(8): 2489-2497, 1991.

45. **Obrenovitch TP, Chen S, Farkas E.** Simultaneous, live imaging of cortical spreading depression and associated cerebral blood flow changes, by combining voltage-sensitive dye and laser speckle contrast methods. *Neuroimage* 45(1): 68-74, 2009.

46. **Park L, Anrather J, Girouard H, Zhou P, Iadecola C.** Nox2-derived reactive oxygen species mediate neurovascular dysregulation in the aging mouse brain. *J Cereb Blood Flow Metab* 27(12): 1908-1918, 2007.

47. **Pellerin L, Pellegri G, Martin JL, Magistretti PJ.** Expression of monocarboxylate transporter mRNAs in mouse brain: support for a distinct role of lactate as an energy substrate for the neonatal vs. adult brain. *Proc Natl Acad Sci U S A* 95(7): 3990-3995, 1998.

48. **Pierre K, Pellerin L.** Monocarboxylate transporters in the central nervous system: distribution, regulation and function. *J Neurochem* 94(1): 1-14, 2005.

49. **Pietrobon D, Moskowitz MA.** Chaos and commotion in the wake of cortical spreading depression and spreading depolarizations. *Nat Rev Neurosci* 15(6): 379-393, 2014.

50. **Popa-Wagner A, Badan I, Walker L, Groppa S, Patrana N, Kessler C.** Accelerated infarct development, cytogenesis and apoptosis following transient cerebral ischemia in aged rats. *Acta Neuropathol* 113(3): 277-293, 2007.

51. **Prince DA, Lux HD, Neher E.** Measurement of extracellular potassium activity in cat cortex. *Brain Res* 50(2): 489-495, 1973.

52. **Scheller D, Kolb J, Tegtmeier F.** Lactate and pH change in close correlation in the extracellular space of the rat brain during cortical spreading depression. *Neurosci Lett* 135(1): 83-86, 1992.

53. **Selman WR, Lust WD, Pundik S, Zhou Y, Ratcheson R.A.** Compromised metabolic recovery following spontaneous spreading depression in the penumbra. *Brain Res* 999(2): 167-174, 2004.

54. **Siesjö BK, Kjällquist A, Pontén U, Zwetnow N.** Extracellular pH in the brain and cerebral blood flow. *Prog Brain Res* 30: 93-98, 1968.

55. **Somjen GG.** Mechanisms of spreading depression and hypoxic spreading depression-like depolarization. *Physiol Rev* 81(3): 1065-1096, 2001.

56. **Sun X, Wang Y, Chen S, Luo W, Li P, Luo Q.** Simultaneous monitoring of intracellular pH changes and hemodynamic response during cortical spreading depression by fluorescence-corrected multimodal optical imaging. *Neuroimage* 57(3): 873-884, 2011.

57. **Tang CM, Dichter M, Morad M.** Modulation of the N-methyl-D-aspartate channel by extracellular H+. *Proc Natl Acad Sci U S A* 87(16): 6445-6449, 1990.

58. **Tombaugh GC.** Mild acidosis delays hypoxic spreading depression and improves neuronal recovery in hippocampal slices. *J Neurosci* 14(9): 5635-5643, 1994.

59. **Tombaugh GC, Somjen GG.** Effects of extracellular pH on voltage-gated Na+, K+ and Ca2+ currents in isolated rat CA1 neurons. *J Physiol* 493(Pt 3): 719-732, 1996.

60. **Tong CK, Chesler M.** Modulation of spreading depression by changes in extracellular pH. *J Neurophysiol* 84(5): 2449-2457, 2000.

61. **Toth P, Tarantini S, Csiszar A, Ungvari Z.** Functional vascular contributions to cognitive impairment and dementia: mechanisms and consequences of cerebral autoregulatory dysfunction, endothelial impairment, and neurovascular uncoupling in aging. *Am J Physiol Heart Circ Physiol* (Jan 1, 2017) doi: 10.1152/ajpheart.00581.2016.

62. **Toth P, Tarantini S, Tucsek Z, Ashpole NM, Sosnowska D, Gautam T, Ballabh P, Koller A, Sonntag WE, Csiszar A, Ungvari Z.** Resveratrol treatment rescues neurovascular coupling in aged mice: role of improved cerebromicrovascular endothelial function and downregulation of NADPH oxidase. *Am J Physiol Heart Circ Physiol* 306(3): H299-H308, 2014.

63. **van Harreveld A.** Compounds in brain extracts causing spreading depression of cerebral cortical activity and contraction of crustacean muscle. *J Neurochem* 3(4): 300-315, 1959.

64. **Varga DP, Puskás T, Menyhárt Á, Hertelendy P, Zölei-Szénási D, Tóth R, Ivánkovits-Kiss O, Bari F, Farkas E.** Contribution of prostanoid signaling to the evolution of spreading depolarization and the associated cerebral blood flow response. *Sci Rep* 6: 31402, 2016.

65. **Voipio J, Kaila K.** Interstitial PCO2 and pH in rat hippocampal slices measured by means of a novel fast CO2/H(+)-sensitive microelectrode based on a PVC-gelled membrane. *Pflugers Arch* 423(3-4): 193-201, 1993.

Figure captions

Figure 1. Variations in the amplitude of the negative direct current (DC) potential shift indicative of spreading depolarization (SD). A, Representative traces of tissue pH and cerebral blood flow (CBF) changes demonstrate signals corresponding to a conventional, fully developed DC signature of an SD (i.e. amplitude of the negative DC shift greater than 5 mV) (left), and a small SD (i.e. amplitude of the negative DC shift smaller than 5 mV) (right). B, Distribution of SD-related DC shift amplitudes in experimental Series 1. Each symbol represents a single SD event (n=62). All three phases of the experiments (i.e. baseline, ischemia and reperfusion) are included.

Figure 2. Correlation analysis considering the amplitude (A-C) and duration (D-F) of the spreading depolarization (SD)-related direct current (DC) potential shift, transient tissue acidosis and hyperemic response, to reveal the impact of aging. A & D, Illustration of the variables considered for the analysis. B, Overview of correlation coefficients delivered by a Pearson two-tailed paradigm ($p<0.05$*, $p<0.01$**) for the association of amplitudes in the young group in *Series 1*, for each of the three subsequent phases of the experiments. Alteration of correlation coefficients is highlighted in bold italic font. C, Representative plots demonstrate the impact of ischemia on the correlation between the amplitude of the DC potential shift indicative of SD and that of the related hyperemia (n=8/11). E, Overview of correlation coefficients delivered by a Pearson two-tailed paradigm ($p<0.05$*, $p<0.01$**) for the association of durations in the young group in *Series 1*, for each of the three subsequent phases of the experiments. Alteration of correlation coefficients is highlighted in bold italic font. F, Representative plots to demonstrate the impact of ischemia on the correlation between the duration of the DC potential shift indicative of SD and that of the related tissue acidosis (n=8/11). Open symbols stand for baseline; black symbols represent ischemia.

Figure 3. Correlation analysis considering the amplitude of the spreading depolarization (SD)-related direct current (DC) potential shift, transient tissue acidosis and hyperemic response, to identify the impact of aging.

A, Illustration of the variables considered for the analysis. B, Overview of correlation coefficients delivered by a Pearson two-tailed paradigm ($p<0.05$*, $p<0.01$**) for the association of amplitudes over baseline in *Series 1*, for each age group. Alteration of correlation coefficients is highlighted in bold italic font. C, Representative plots demonstrate the impact of age on the correlation between the amplitude of the DC potential shift indicative of SD and that of the related hyperemia (n=8/age group).

Figure 4. Correlation analysis and relative changes considering the duration of the spreading depolarization (SD)-related direct current (DC) potential shift, transient tissue acidosis and hyperemic response, to identify the impact of aging. A, Illustration of the variables considered for the analysis. B, Overview of correlation coefficients delivered by a Pearson two-tailed paradigm ($p<0.05$*, $p<0.01$**; n=8-11/group) for the association of durations over ischemia in *Series 1*, for each age group. C, Duration of SD-related acidosis and hyperemia relative to the duration of the DC potential shift (taken as 100 %) in *Series 1* during ischemia. Horizontal bars are color-coded according to Panel A (i.e. green: DC potential shift, blue: acidosis, red: hyperemia). Relative values (bold) were derived from the mean absolute values given in parentheses (mean±stdev; n=8-11/ group). A one-way analysis of variance (ANOVA) followed by a Fisher post hoc test was used for statistical analysis (*Young ischemia*, F=10.962**; Old ischemia, F=13.144**). Levels of significance are given as $p<0.01$**, vs. DC potential; $p<0.01^{\#\#}$, vs. acidosis.

Figure 5. Images illustrate a spreading depolarization (SD) event that was initiated at the stimulating glass capillary (S in A_1), propagated radially, but aborted halfway within the field of view (dotted white line in A_1 indicates the zone where SD came to a halt). A_2 demonstrates an image of NR fluorescence captured in the field of view prior to SD elicitation. A_3 and A_4 are pseudo-colored perfusion maps based on laser speckle contrast images to demonstrate the cortical area involved in the propagation of the aborting SD (i.e. hyperemia denoted by warm colors spatially extends as far as the SD propagated). B, Traces of Neutral Red (NR) fluorescence intensity and cerebral blood flow (CBF) taken at three regions of interest (ROI) shown in A_1, and the direct current (DC) potential signature of a small SD (electrode "E" is shown in A_1). ROI3

(indicated in A_1) was positioned as near the glass capillary electrode (E in A_1) as the pial vascular architecture allowed. Note that the extinguishing SD appears as a small DC shift at the recording site.

Figure 6. Association between tissue pH prior to spreading depolarization (SD) and the amplitude of the direct current (DC) potential shift with SD. A, Illustration of the origin of data sets analyzed. B, Tissue pH prior to SD events evoked during baseline in *Series 1*, events sorted on the basis of DC shift amplitude. C, Correlation coefficients delivered by a Pearson two-tailed paradigm ($p<0.05$*, $p<0.01$**; n=7/8) for the association of variables in the young group in *Series 1*, for each of the three subsequent phases of the experiments. The impact of ischemia on the correlation coefficient is highlighted in bold italic font. D, Graphic illustration of the impact of ischemia on the correlation between tissue pH and the amplitude of the SD-related DC shift. Open symbols stand for baseline; black symbols represent ischemia.

Figure 7. Conceptual overview of the causal sequence of associations between the amplitudes of variables, as proposed on the basis of the current analyses.

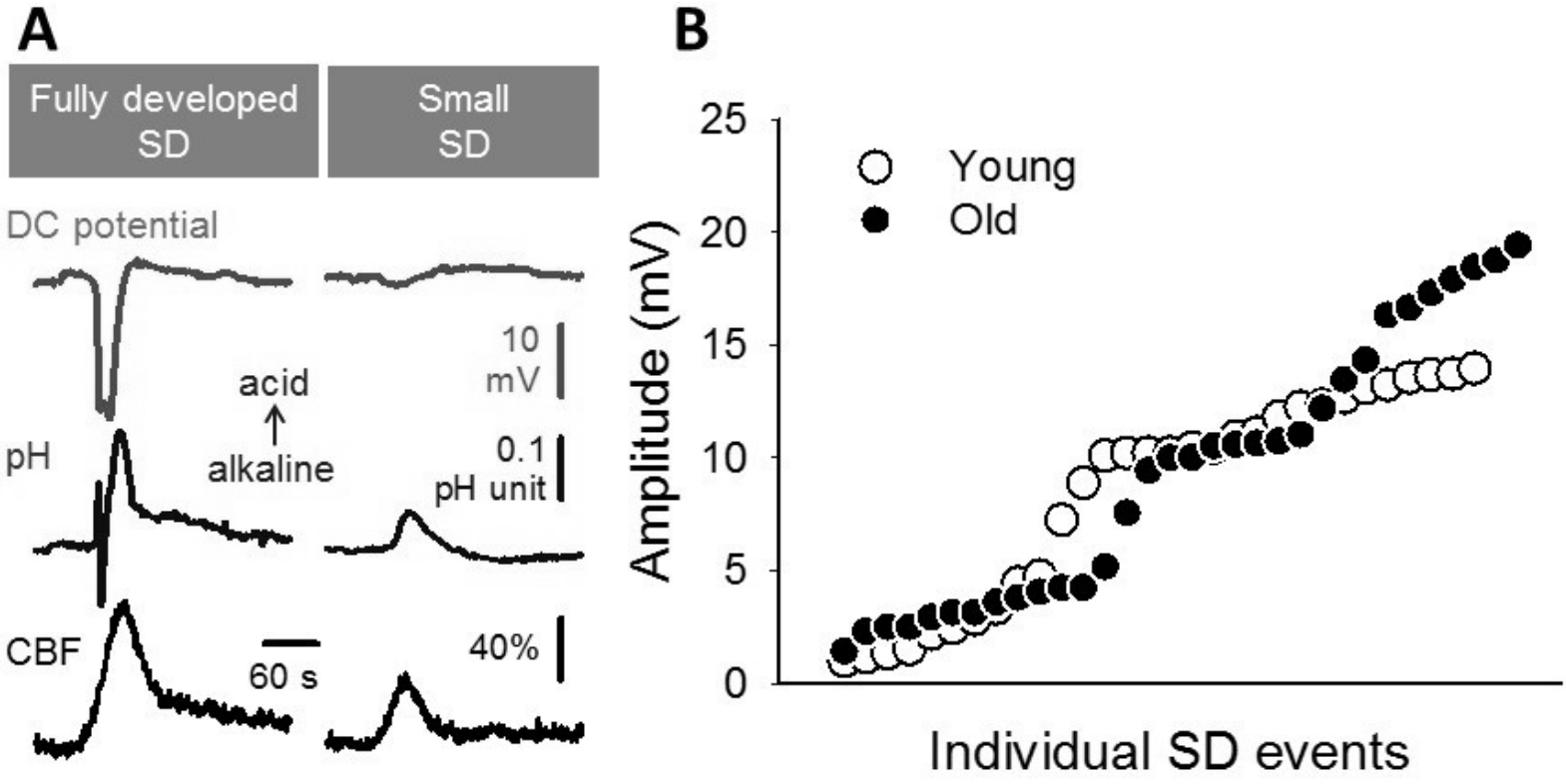
A
Fully developed SD
Small SD
DC potential
10 mV
acid
alkaline
pH
0.1 pH unit
CBF
60 s
40%
B
Young
Old
Amplitude (mV)
25
20
15
10
5
0
Individual SD events

A

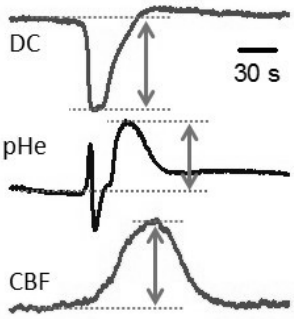

B

Amplitude	Baseline	Ischemia	Reperfusion
DC shift & acidosis	0.782*	0.789**	0.615
hyperemia & DC shift	0.819*	***0.236***	***-0.133***
hyperemia & acidosis	0.871**	***0.429***	***-0.019***

C

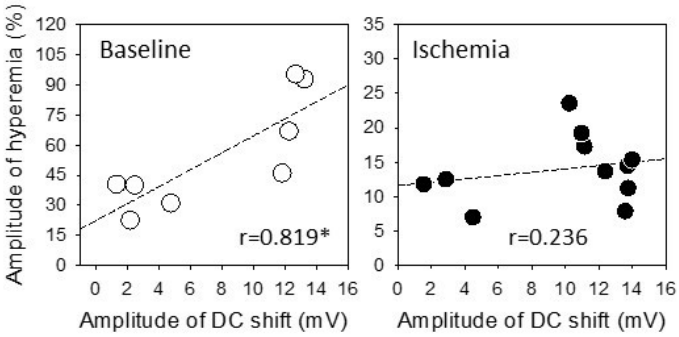

D

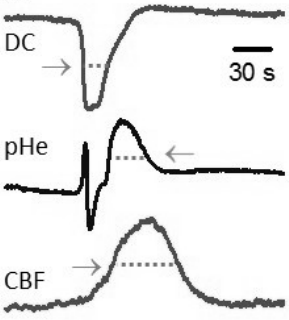

E

Duration	Baseline	*Ischemia*	Reperfusion
DC shift & acidosis	0.157	***0.935****	0.071
hyperemia & DC shift	0.176	***0.634****	-0.044
hyperemia & acidosis	0.556	***0.681****	0.067

F

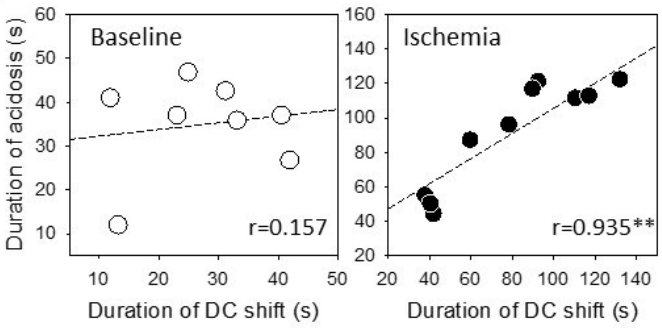

A Baseline

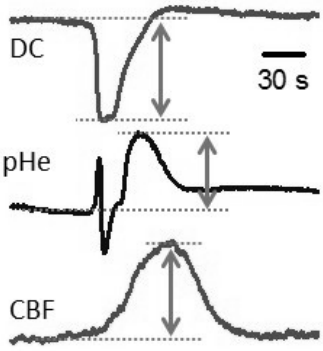

B

Amplitude	Young	Old
DC shift & acidosis	0.782*	0.998**
hyperemia & DC shift	0.819*	***0.221***
hyperemia & acidosis	0.871**	***0.249***

C

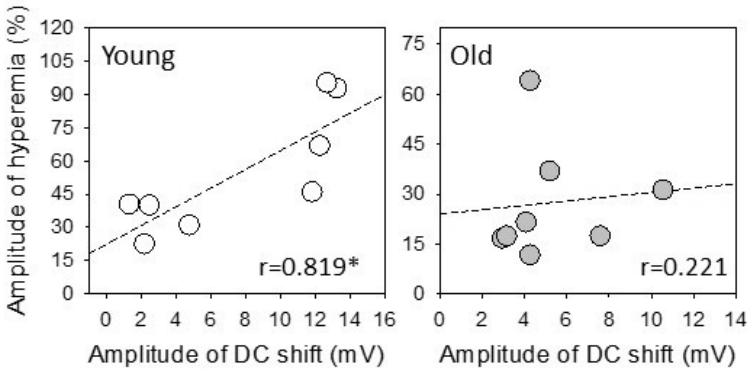

A

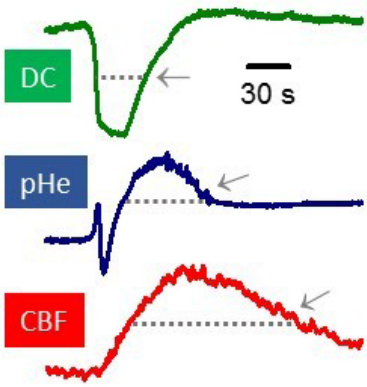

B

Ischemia

Duration	Young	Old
DC shift & ***acidosis***	0.935**	***0.482***
hyperemia & DC shift	0.634*	0.657*
hyperemia & ***acidosis***	0.681*	***0.286***

C

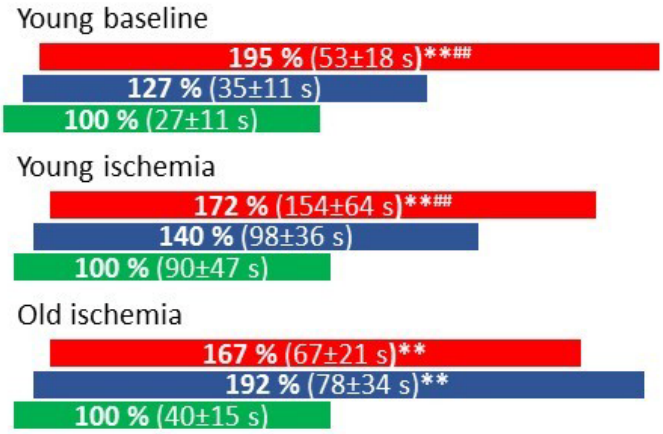

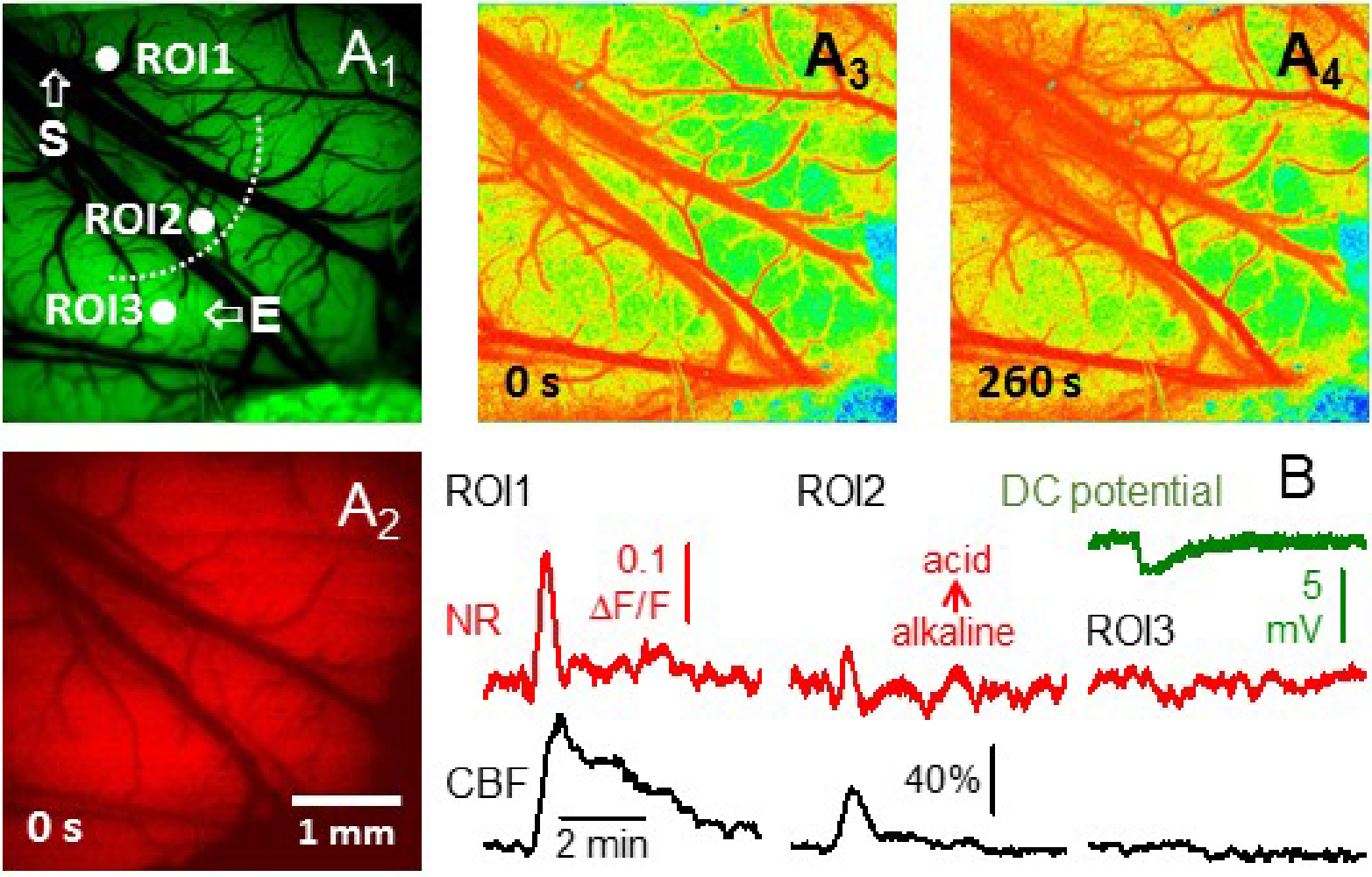
ROI1
A1
S
ROI2
ROI3
E
A3
0 s
A4
260 s
A2
0 s
1 mm
ROI1
ROI2
DC potential
B
0.1
ΔF/F
NR
acid
alkaline
ROI3
5
mV
CBF
2 min
40%

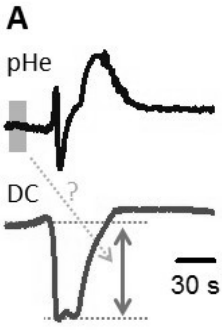

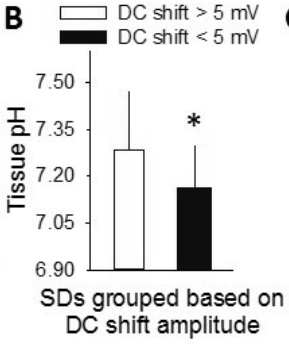

C Association between tissue pH prior to SD occurrence & DC amplitude

Phase	r
Baseline	0.909**
Ischemia	***0.244***
Reperfusion	0.739*

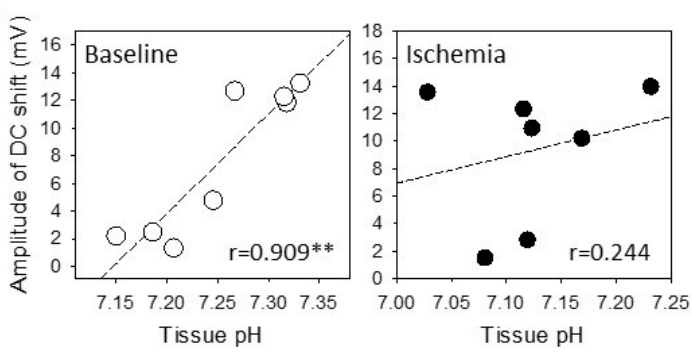

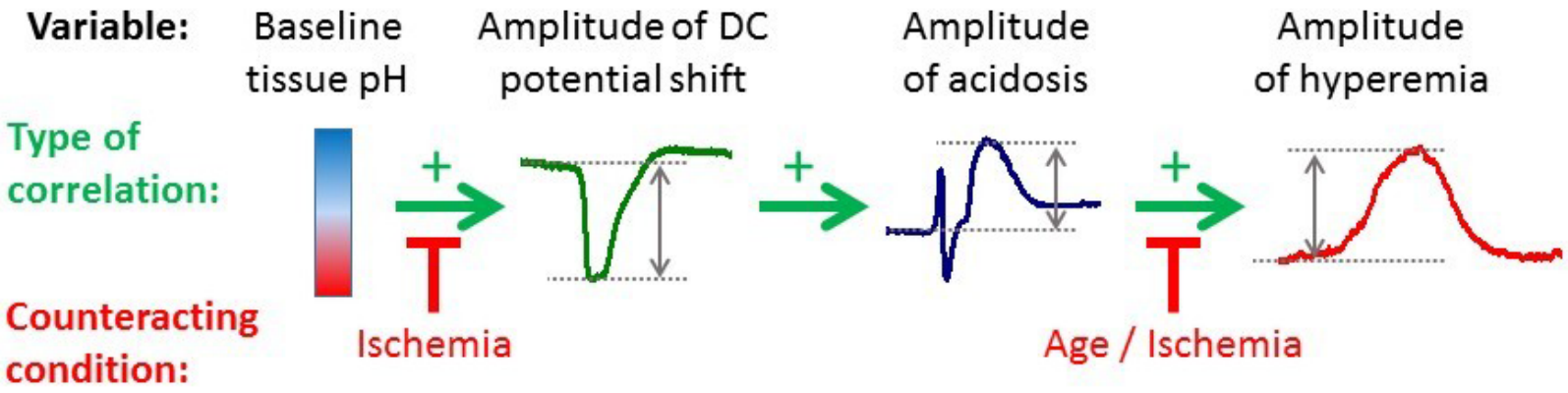
Variable:
Baseline tissue pH
Amplitude of DC potential shift
Amplitude of acidosis
Amplitude of hyperemia
Type of correlation:
+
+
+
Counteracting condition:
Ischemia
Age / Ischemia